Life cycle of a tungsten cold field emitter

K. S. Yeong and J. T. L. Thong[a)]
Department of Electrical and Computer Engineering, Faculty of Engineering, National University of Singapore, 4 Engineering Drive 3, Singapore 117576, Singapore

(Received 20 November 2005; accepted 23 February 2006; published online 25 May 2006)

This paper studies a tungsten cold field emitter throughout its life cycle. The field emission properties and corresponding tungsten emitter evolution throughout its life cycle fall into three distinct regions which are discussed. It was found that adsorbate dynamics affect field emission current stability significantly, while adsorbate induced current instability showed different behaviors in different regions of the life cycle. It was found that emitter failure at the end of the lifetime was due to adsorbate related nanoprotrusion buildup on the emitter surface, a failure mechanism that is different from models previously reported in the literature. The buildup process of this nanoprotrusion and how it initiates arcing and destroys the tungsten tip are reported and discussed.
 [DOI: 10.1063/1.2197267]

I. INTRODUCTION

The field emission properties of tungsten tips have been studied in great detail since the 1930s. The theory of field emission,[1–3] the resolution of field emission microscopy,[4,5] surface science related issues,[2] and the performance of tungsten tips as an electron source[6,7] have been well formulated, developed, and documented after extensive effort expended by many researchers. Good reviews on the early works in field emission can be found in Refs. 2 and 3. At the present time, tungsten tips are widely used as electron sources operating in the thermal-field emission and Schottky emission regimes. On the other hand, despite its early introduction in commercial electron microscopes, the cold field emission cathode is rather less popular, although it has the potential for higher brightness and lower energy spread. This is largely due to difficulties faced in maintaining emission current stability and the likelihood of catastrophic failure at the end of its lifetime.

Poor emission stability is well known to be due to the effect of adsorbates and surface atom dynamics. Adsorbates form a surface layer on the emitter tip which changes the work function of the emission tip and thus affects the emission current significantly. The dynamics of adsorbates on the emitter surface cause flicker noise in the emission current.[8,9] On the other hand, sputtering of the emitter tip by residual gas ions causes spikelike noise in emission current.[10] Yu *et al.* managed to improved emission current stability by engineering their emitter tip to reduce surface atom dynamics through carburization of the tungsten tip and controlled field ion desorption to form a flat (111) facet at the tip end.[11,12]

Catastrophic failure of tungsten cold field emitters is often due to residual gas ion bombardment which roughens the emitter surface, causing excessive current emission from surface microprotrusions, which finally leads to arc destruction of the tip.[13] Another failure mechanism proposed by Dyke *et al.* is thought to occur at high current densities in the order of 10^8 A/cm^2, where the tungsten emission tip is resistively heated up to high temperatures. At high temperatures and electric fields, arcing initiates and destroys the emitter.[14]

While many studies have been conducted on tungsten cold field emitters, these have focused on specific field emission characteristics or phenomena, rather than the evolution of the field emission throughout the lifetime of a cathode. In this paper, we study the life cycle of a tungsten cold field emitter starting from a fresh electrochemically etched tungsten tip to the end of its life to provide a framework to link the extant knowledge of cold field emission and to understand the causes of emission current instability in cold field emitters. Current stability, current voltage behavior, and field emission microscopy were mainly used in a correlated manner to perform the studies. The evolution of the tungsten tip that affects the field emission characteristics and a failure mechanism which causes arc destruction of the emitter are identified and discussed. We identified and captured a process in which adsorbates build up and which finally leads to the initiation of arcing. This process is related to adsorbate nanoprotrusions, a failure mechanism that is different from previously suggested models.

II. SETUP

Figure 1 shows the UHV field emission characterization chamber. The chamber has a titanium sublimation pump in addition to a dual-stage turbopump backed by a dry pump and is capable of reaching a base pressure of 10^{-10} mbar. The field emitter is loaded via a loadlock onto a rotatable stage at the center of the chamber, facing a hole-extraction anode and a phosphor screen. The setup has the ability to perform current voltage (*I-V*) measurements, current stability (*I-t*) measurements, field emission microscope (FEM) imaging, and field electron energy distribution (FEED) measurement with a sector energy analyzer (Focus Electronics CSA 200). All data acquisition is carried out under computer control. FEM images are recorded using a digital video camera recorder at 30 fps.

[a)]Author to whom correspondence should be addressed; electronic mail: elettl@nus.edu.sg

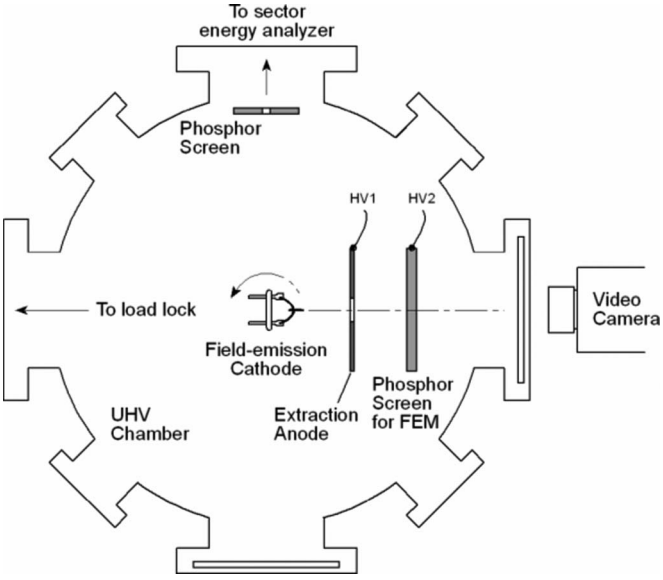

FIG. 1. Field emission characterization system.

Field emission tips are fabricated from electrochemically etched polycrystalline tungsten wire. Typical as-etched tip radii are around 50 nm. The tip is spot-welded on a filament loop on a commercial cathode base. Annealing of the field emitter is carried out by resistive heating of the filament loop. The temperature of the field emitter is measured at the spot-weld using a disappearing-filament pyrometer. Due to the thermal gradient and radiative losses along the tip shank, the temperature at the tip apex is estimated to be about 200–300 °C lower than the spot-welded region for measured temperatures of around 1000 °C.

III. RESULT AND DISCUSSION

Field emission characterization was carried out at a pressure of about 5×10^{-9} mbar. Working at this high chamber pressure reduces the tungsten cold field emitter lifetime significantly to a few hours per cycle, thereby shortening the experimental observation time frame. The field emission current from an as-etched tip is very unstable due to the extant tungsten oxide layer and surface roughness and very often leads to arcing if the emission current is greater than 1 μA. Annealing of the fresh tungsten tip by heating from room temperature to high temperatures desorbs the tungsten oxide layer and at the same time initiates surface diffusion which results in a clean and smooth tungsten tip. Annealing at 2400 °C (measured at spot-welded region) or greater desorbs

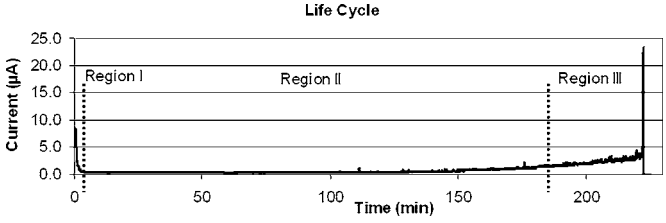

FIG. 2. Emission current behavior of tungsten cold field emitter throughout its life cycle at constant anode voltage right after annealing at 2400 °C.

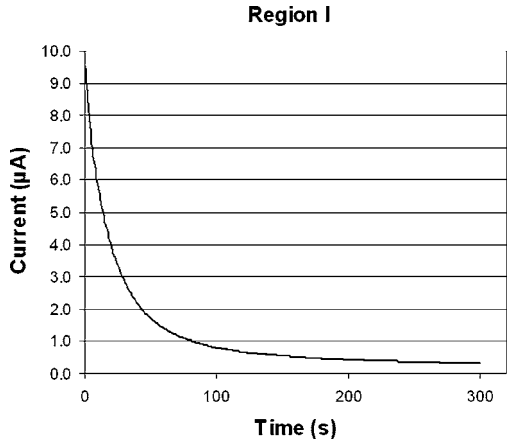

FIG. 3. *I-V* characteristic of first 30 s of region I right after annealing at 10 kV anode potential. Data were taken at 100 ms sampling rate.

all surface contaminants. The FEM image of the flashed tungsten surface corresponds to the crystal orientation of the tungsten tip as shown in Fig. 4(a).

Immediately following the annealing at 2400 °C, the emission current decreased rapidly for a few minutes before it stabilized at a current that is about two orders of magnitude lower. The stable region can last for a few hours, depending on the vacuum level and the emission current. Beyond this, the emission current starts to fluctuate with increasing intensity until a point where the emission current ceased abruptly. These three distinct regimes of emission current behavior following annealing are shown in Fig. 2 and are divided into regions I, II, and III which span the life cycle of the emitter. The corresponding FEM images exhibit distinct characteristics in each region.

A. Region I

Following annealing at 2400 °C, the emission current at constant electric field decreased rapidly over a few minutes until it stabilized at a current that is about one to two orders of magnitude lower as shown in Fig. 3.

Figure 4 shows the changes in the FEM pattern over the duration of region I. Figure 4(a) shows the FEM pattern of

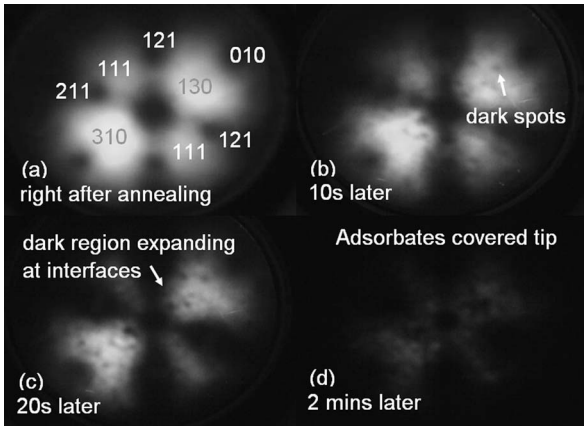

FIG. 4. Changes in FEM pattern across region I, extracted from the video recording. Extraction anode and phosphor screen were biased at 10 and 2 kV, respectively.

the clean tungsten surface right after annealing which corresponds to the crystal structure of the emission tip.[15] Emission from closely packed crystal facets such as (110), (211), and (121) appear as dark regions, whereas less densely packed facets such as (310) and (111) give rise to bright regions in the FEM pattern. Figures 4(b)–4(d) show the subsequent FEM pattern changes in region I. The high emission regions progressively became smaller and dimmer while losing traces of symmetry toward the end of region I. The changes in emission current and FEM pattern are due to the increase in work function of the emitting surfaces resulting from electronegative adsorbate molecules being adsorbed on the emission surface. Such adsorbate molecules originated from residual gases in the vacuum and from desorption by electron bombardment of the anode surface. The readsorption process of these molecules on emission surface is assisted by the strong electric field directing the ionized molecules to the emission tip. Adsorbate molecules are likely to be H_2, CO, CO_2, and H_2O which are the main gas components in an UHV chamber.[16]

An interesting phenomenon is seen in Figs. 4(b) and 4(c). Inside the bright emission region, discrete dark spots appear in the middle of the high emission region. The dark spots are likely to arise from individual adsorbate molecules being adsorbed on the emitter surface. These adsorbates increased the local work function and thus induced dark spots on the bright background. The overall decrease in the emission current with time and gross FEM pattern changes are due to the collective behavior of such individual events. From a different perspective, it shows that FEM is capable of resolving at least individual molecules resting on a smooth emission surface.

The progressive decrease in emission current in region I is the first technical challenge if the emission current from a cold field emitter were to be maintained. It can be reduced by improving the vacuum, anode cleanliness, and the emitter tip to anode geometry. Martin *et al.* were able to maintain the emission current right up to 1000 h by enclosing the cathode with a tubular anode to trap secondary electrons.[13] Secondary electron trapping reduced ionization of residual gas molecules and electron impact desorption of surface gas molecules significantly and thus reduced the rate of adsorption on the emitter surface as well.

B. Region II

Region II represents a period of stable average emission current after the rapid current drop in region I. The emission current drifted gradually around an average current that is about one to two orders of magnitude lower than the initial current following annealing. As adsorbates fully covered the emission tip, the emission current reached a plateau (Fig. 5). The emission current is found to be quite stable with very small current drift. Emission current noise is mainly flicker noise and occasionally spikelike noise due to adsorbate dynamics on the emitter surface.[10] The standard deviation in the current throughout the 100 s is 2.9%. This stable region can last for a few hours, depending on the magnitude of

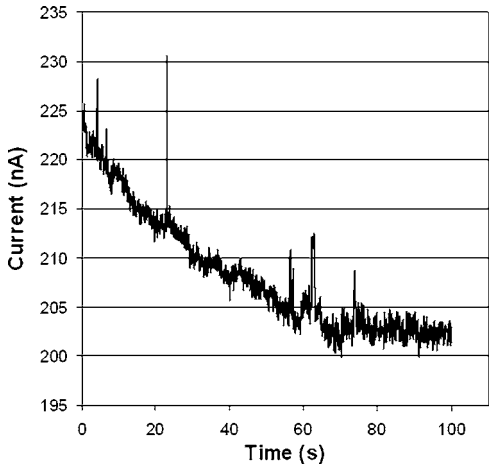

FIG. 5. Emission current in region II at 10 kV anode potential, starting at 300 s following annealing. Emission current is much more stable compared to regions I and III. Data were taken at 100 ms sampling intervals.

emission current and vacuum level before the emission current and emission noise starts to increase as we enter region III.

A typical FEM pattern in region II is shown in Fig. 6. The FEM pattern shows no symmetry since emission is from the layer of adsorbates on the tip. The pattern also shows that the emission spots are distributed over the surface. The emission spots are likely to have arisen from adsorbate clusters, whereas the bright center rim was due to adsorbate molecules that adsorbed on the edge of (110) facet. Most emission spots were stationary with constant brightness in the FEM pattern although some of them were blinking (brightness fluctuating) most of the time. Occasionally, a bright emission spot will appear from nowhere for a short while before it disappears and reappears again at the same position. These emission-spot characteristics correspond to the adsorbate-molecule dynamics on the tip surface. The bright spot may appear as a round spot or as a doublet, possibly FEM patterns of a single adsorbate molecule.[17,18] We observed the correlation of the appearance and disappearance of bright spots to spikelike emission current noise as shown in Fig. 6. One of the possible origins of the spikelike noise is emitter surface bombardment by gas molecules in the vacuum.[10] On the other hand, flicker noise has been known to be due to surface diffusion of tungsten atoms during thermal-field emission, adsorbate-molecule diffusion,

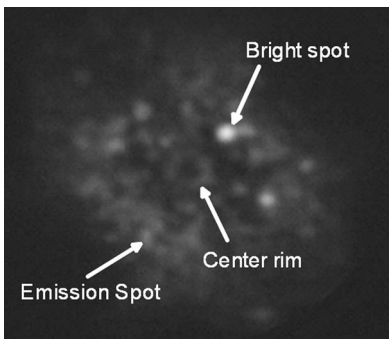

FIG. 6. FEM pattern in region II. The picture frame is extracted from the recorded movie at 30 fps.

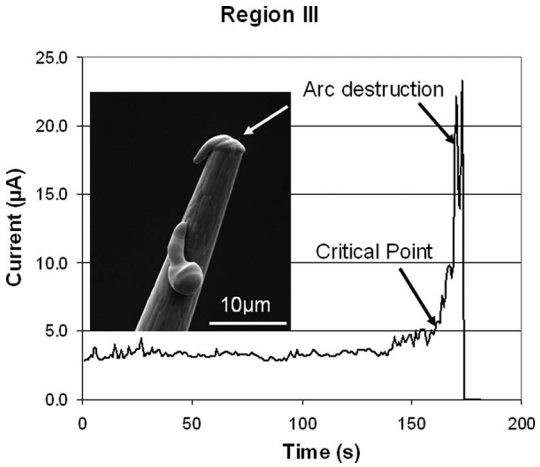

FIG. 7. *I-t* characteristic of region III over the final 175 s before the tip died. Data were taken at 100 ms sampling rate. The inset shows the tungsten tip after arc destruction.

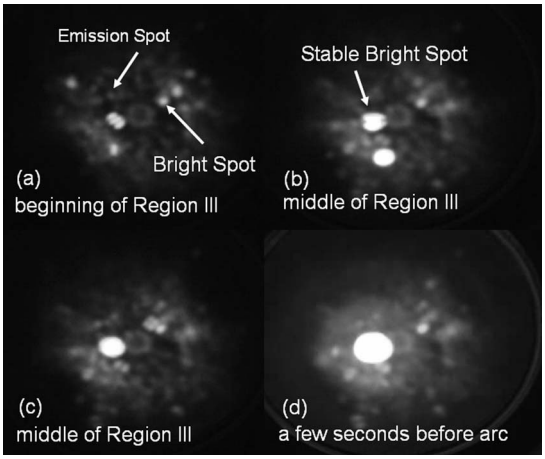

FIG. 8. FEM pattern of adsorbate nanoprotrusion buildup process in region III at constant applied field.

adsorbate-molecule flip-flop,[8,9,19] and likely emission field-current induced rotation, vibration, and desorption of adsorbate molecules. The brightness fluctuation of stationary emission spots corresponds to the flicker noise shown in Fig. 5. The fluctuation is likely to be due to emission field-current induced elementary dynamic vibration of the adsorbate molecules.

A tungsten tip covered with adsorbates has a higher work function compared to a clean tungsten tip. The change is evident from the Fowler-Nordheim (FN) plots of a clean tungsten tip and the same adsorbate-covered tungsten tip. The work function is estimated to increase by 0.45 eV, consistent with earlier work on CO adsorbed tungsten tips.[20]

C. Region III

The starting point of region III is chosen roughly to be the time when the emission current has increased by about one order of magnitude compared to the emission current at the start of region II. The increase in current corresponds to an increase in the number of extraordinarily bright emission spots as shown in Fig. 8(a). Emission gradually increased throughout region III until it reach a critical point where the current increased rapidly which then triggered a catastrophic event that caused the emission current to cease abruptly as shown in Fig. 7.

The evolution of the FEM pattern across region III is shown in Fig. 8. Figures 8(a)–8(c) were FEM pattern observed in the beginning and middle regions of region III. Figure 8(d) shows the pattern just before the emission current ceased abruptly. Region III started with a few bright spots which were quite stable. These bright spots grew and became more stable and brighter until the end, where a single stable bright spot dominated the emission process. This spot continued growing before it suddenly burst and the FEM image disappeared. We believe that the stable bright spots were clusters of adsorbate molecules or adsorbate-tungsten compound that gathered at a favorable site on the emission surface. The favored adsorbate clustering sites are typically damaged surface regions created by energetic ion sputtering throughout the tip lifetime. Since adsorbate molecules are physically adsorbed on the emitter surface, they should be mobile enough to be driven by the electric field to form molecular clusters, analogous to the formation of buildup nanostructures in thermal-field emission.[21,22] Small clusters are metastable and often decay and disappear as manifested by the disappearance of the corresponding bright spot in the FEM pattern. However, once a cluster has reached a critical size, it is stable and continues to grow until catastrophic destruction. These clusters are in the form of nanometer-sized protrusion on the emission surface. Although the stable bright spot appears large compared to the background emission pattern in the FEM, the physical size of the nanoprotrusion should be just about a nanometer to at most a few nanometers. Additional magnification of the nanoprotrusion FEM compared to its background is due to local magnification of nanoprotrusion on a smooth surface.[5]

The stable adsorbate nanoprotrusion dominated the field emission process and exhibited high angular current density (small beam divergence) as shown in Fig. 8(d). High emission current from nanoprotrusions compared to their background is mainly due to local field enhancement of the nanoprotrusions. The high angular current density is due to the electrostatic field around the huge tungsten shank inserting a compression force to the electron trajectory as in the case of an atomic nanotip.[21,23] By lowering the emission cur-

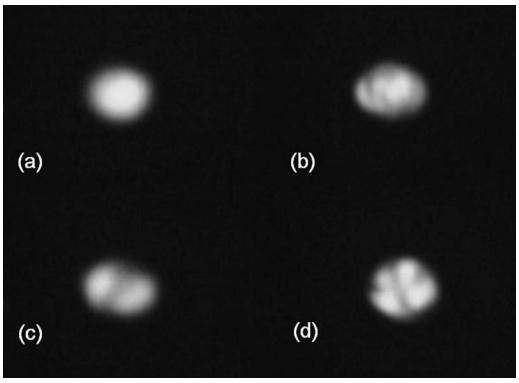

FIG. 9. FEM pattern of ultrasharp adsorbate nanoprotrusion at about 200 nA emission current. The anode was biased at ~3500 V, while phosphor screen at 2000 V.

rent below 1 μA, the adsorbate nanoprotrusion can field emit for many hours without leading to arcing. The FEM patterns of adsorbate nanoprotrusion at low currents are shown in Fig. 9. The images show that the nanoprotrusion continuously changes its emission pattern, likely to be due to field-induced desorption or current-induced rotation/vibration of the adsorbate molecule at the tip of the nanoprotrusion. The most common emission patterns observed are the nonsymmetrical pattern (9b), but occasionally rounded-spot (9a), doublet (9c), and quadruplet (9d) patterns are also seen. As discussed in the literature, doublets and quadruplets are considered to be related to single-molecule emission. Brodie also showed that atomic resolution in FEM is possible if the tip radius is small enough.[24] Thus, in this case, we believe that the emission pattern is due to the nanoprotrusion that forms an ultrasharp tip, probably with molecular dimensions.

Ultrasharp nanoprotrusion emission current was not stable except at very low currents of typically a few nanoamperes. Current fluctuations of around 50% (standard deviation) were observed at emission currents of a few hundred nanoamperes, whereas at a few tens of nanoamperes, emission noise reduced to $\sim$10%, suggesting good emission stability in the lower emission current range and is worth examining more closely. The emission exhibits random fluctuations at high currents and steplike current jumps at low currents. Thus, adsorbate nanoprotrusion shows field emission properties such as small beam divergence, steplike current jumps, and good stability at low currents, similar to buildup single atom nanotips studied by Binh *et al.*[21]

Charbonnier *et al.* investigated electrical breakdown across narrow gaps between metal electrodes in high vacuum and found that the most significant factors limiting the stability of the gap are (1) excessive heating of a cathode protrusion by emission current, (2) excessive electron beam power density at the anode, (3) excessive ion bombardment of cathode protrusions, and (4) excessive electrostatic stress at either electrode surfaces.[25,26] In studying tungsten cold field emitters which normally involves a large distance between the anode and the cathode, in an UHV environment, factors 1 and 4 are the main causes of electrical breakdown.

Indeed, the most common tungsten cold field emitter failure mechanisms reported previously involve excessive heating of cathode. Dyke *et al.* discovered that field emission at very high current densities ($\geqslant 10^8$ A/cm^2) induces significant resistive heating at the emitter tip. Excessive heating at high currents and high electric fields leads to emitter arcing destruction.[14,27] Martin *et al.* proposed another arcing mechanism that occurs at a lower emission current density. In their experiment, He ions ionized by the electron beam sputtered the emitter surface and thus increased the surface roughness and emission current. Surface projections emitting high current densities eventually "burn off" and cause local arcing that might spread to the entire tungsten tip.[13]

In our case, at the end of region III, the buildup of adsorbate nanoprotrusion was the cause of the arc destruction of the tungsten field emitter. In this process, a high emission current density from an adsorbate nanoprotrusion resistively heats up the nanoprotrusion to result in even higher emission currents. This positive feedback effect triggers rapid current rise (as shown in Fig. 7) after the critical point until the nanoprotrusion vaporizes. The vaporized material under an intense electron beam irradiation and a strong electric field immediately triggers localized arcing which can spread to the entire emitter tip and lead to its destruction. Nanoprotrusions can be easily evaporated by heating the tungsten filament to just 800 °C. This supports the claim that such nanoprotrusions are adsorbate clusters since they evaporate at relatively low temperatures.

IV. CONCLUSION

We have studied the field emission properties of a tungsten cold field emitter throughout its life cycle. The emission current characteristics throughout the life span are shown to have three distinct regions which were classified as regions I, II, and III. In region I, emission current decreases rapidly immediately following annealing at high temperatures due to field-assisted adsorption on the clean emission surface. Adsorbate molecules originate from residual gases and desorption from the anode surface. The emission current is found to decrease by about two orders of magnitude. In region II, the emission current enters a stable region. Emission current is quite stable with small flicker noise and occasional spikelike noise. Such stable emission current can last for a few or many hours, depending on the current and vacuum level. In this region, field emission is from multilayers of adsorbates covering the tungsten tip. In region III, emission current and emission noise start to increase due to the formation of adsorbate nanoprotrusions. The stable adsorbate nanoprotrusions dominate the field emission current and cause resistive heating that eventually triggers catastrophic arcing and tip destruction.

ACKNOWLEDGMENT

This project is supported by a NUS research Grant No. R-263-000-250-112 and a grant from A*STAR.

[1] R. H. Fowler and L. W. Nordheim, Proc. R. Soc. London **A119**, 173 (1928).
[2] W. P. Dyke and W. W. Dolan, *Field Emission*, Advances in Electronics and Electron Physics Vol. 8 (Academic, New York, 1956).
[3] R. Gomer, *Field Emission and Field Ionization* (Harvard University Press, Cambridge, MA, 1961), Chap. 4.
[4] R. Gomer, J. Chem. Phys. **20**, 1772 (1952).
[5] D. J. Rose, J. Appl. Phys. **27**, 215 (1956).
[6] L. W. Swanson and N. A. Martin, J. Appl. Phys. **46**, 2029 (1975).
[7] A. V. Crewe, D. N. Eggenberger, J. Wall, and L. M. Welter, Rev. Sci. Instrum. **39**, 576 (1968).
[8] Ch. Kleint, Surf. Sci. **25**, 394 (1971).
[9] Ch. Kleint, Surf. Sci. **200**, 472 (1988).
[10] K. Ashihara, H. Nakane, and H. Adachi, J. Vac. Sci. Technol. B **16**, 1180 (1998).
[11] M. L. Yu, B. W. Hussey, H. S. Kim, and T. H. P. Chang, J. Vac. Sci. Technol. B **12**, 3431 (1994).
[12] M. L. Yu, B. W. Hussey, E. Kratschmer, and T. H. P. Chang, J. Vac. Sci. Technol. B **13**, 2436 (1995).
[13] E. E. Martin, J. K. Trolan, and W. P. Dyke, J. Appl. Phys. **31**, 782 (1960).
[14] W. P. Dyke, J. K. Trolan, E. E. Martin, and J. P. Barbour, Phys. Rev. **91**, 1043 (1953).
[15] F. Ashworth, *Advances In Electronics* (Academic, New York, 1951), Vol. 3.
[16] N. Saitou and S. Yamamoto, Surf. Sci. **5**, 374 (1980).
[17] J. Melmed and E. W. Müller, J. Chem. Phys. **29**, 1037 (1958).
[18] J. A. Becker, Adv. Catal. **7**, 136 (1955).

[19]L. W. Swanson, Surf. Sci. **70**, 165 (1978).
[20]P. L. Young and R. Gomer, J. Chem. Phys. **61**, 4955 (1974).
[21]V. T. Binh, N. Garcia, and S. T. Purcell, *Electron Field Emission from Atom-Sources: Fabrication, Properties, and Applications of Nanotips*, Advances in Imaging and Electron Physics Vol. 95 (Academic, New York, 1996).
[22]J. Dou, W. J. Shang, and Z. W. Chen, J. Vac. Sci. Technol. B **22**, 597 (2004).
[23]M. L. Yu and T. H. Philip Chang, Appl. Surf. Sci. **146**, 334 (1999).
[24]I. Brodie, Surf. Sci. **70**, 186 (1978).
[25]F. M. Charbonnier, C. J. Bennette, and L. W. Swanson, J. Appl. Phys. **38**, 627 (1967).
[26]F. M. Charbonnier, C. J. Bennette, and L. W. Swanson, J. Appl. Phys. **38**, 634 (1967).
[27]W. P. Dyke, J. K. Trolan, W. W. Dolan, and C. J. Barnes, J. Appl. Phys. **24**, 570 (1953).